

Circular RNA profiling in the oocyte and cumulus cells reveals that circARMC4 is essential for porcine oocyte maturation

Zubing Cao^{1,*}, Di Gao^{1,*}, Tengeng Xu¹, Ling Zhang¹, Xu Tong¹, Dandan Zhang¹, Yiqing Wang¹, Wei Ning¹, Xin Qi¹, Yangyang Ma¹, Kaiyuan Ji¹, Tong Yu¹, Yunsheng Li¹, Yunhai Zhang¹

¹Anhui Province Key Laboratory of Local Livestock and Poultry, Genetical Resource Conservation and Breeding, College of Animal Science and Technology, Anhui Agricultural University, Hefei 230036, China

*Equal contribution

Correspondence to: Yunhai Zhang; email: yunhaizhang@ahau.edu.cn

Keywords: circular RNA, pig, cumulus cells, oocytes, meiotic maturation

Received: March 31, 2019

Accepted: September 21, 2019

Published: September 28, 2019

Copyright: Cao et al. This is an open-access article distributed under the terms of the Creative Commons Attribution License (CC BY 3.0), which permits unrestricted use, distribution, and reproduction in any medium, provided the original author and source are credited.

ABSTRACT

Thousands of circular RNAs (circRNAs) have been recently discovered in cumulus cells and oocytes from several species. However, the expression and function of circRNA during porcine oocyte meiotic maturation have been never examined. Here, we separately identified 7,067 and 637 circRNAs in both cumulus cells and oocytes via deep sequencing and bioinformatic analysis. Further analysis revealed that a faction of circRNAs is differentially expressed (DE) in a developmental stage-specific manner. The host genes of DE circRNAs are markedly enriched to multiple signaling pathways associated with cumulus cell function and oocyte maturation. Additionally, most DE circRNAs harbor several miRNA targets, suggesting that these DE circRNAs potentially act as miRNA sponge. Importantly, we found that maternal *circARMC4* knockdown by siRNA microinjection caused a severely impaired chromosome alignment, and significantly inhibited first polar body extrusion and early embryo development. Taken together, these results demonstrate for the first time that circRNAs are abundantly and dynamically expressed in a developmental stage-specific manner in cumulus cells and oocytes, and maternally expressed *circARMC4* is essential for porcine oocyte meiotic maturation and early embryo development.

INTRODUCTION

Oocyte meiotic maturation is the last stage of oogenesis and is the indispensable prerequisite for fertilization, preimplantation development of the embryo and even term development [1]. In mammals, oocytes meiotically arrested at the prophase I stage have to undergo germinal vesicle (GV) breakdown and subsequent first polar body extrusion to reach the metaphase stage of meiosis II (MII). Under the physiological conditions, oocytes are typically enclosed in several layers of cumulus cells, thus its meiotic maturation is normally accompanying with the correct execution of cumulus cell function. Indeed, numerous studies showed that the reciprocal communications between the oocyte and its encircling cumulus cells are critical not only for the acquisition of both meiotic and developmental competence of oocytes

but also for the execution of cumulus cell function [2–4]. Therefore, the identification of novel molecules expressed in either cumulus cells or oocytes could be informative in elucidating their relative contributions to oocyte meiotic maturation and development.

Although many efforts have been made to improve the oocyte maturation *in vitro* in pigs, its meiotic and developmental capacity is still suboptimal relative to that under the physiological states [5, 6]. This may be due to the imperfectness of *in vitro* culture conditions currently used that cannot achieve the optimal maturational outcomes, and there is inadequate information regarding the unique molecular mechanisms of porcine oocyte meiotic maturation [7, 8]. It is known that oocyte maturation is intricately regulated by cumulus cell or oocyte itself derived non-coding RNAs, such as

microRNA (miRNA) [9–13], endogenous small interference RNA (siRNA) [14] and long non-coding RNA (lncRNA) [15]. Recently, circular RNA (circRNA) has received increasing attention in multiple biological research fields. CircRNA, formed by back-splicing of pre-mRNA transcripts, is a novel class of non-polyadenylated, single-stranded, covalently closed and long noncoding RNAs. Previous studies indicated that circRNA is mainly derived from exons, introns, intergenic regions [16], and is widely distributed on the chromosomes in animal cells [17–19]. CircRNA is discovered to frequently exert different molecular functions, such as transcriptional regulation, microRNA and RNA binding protein sponge, and mRNA trap [20]. It is worthy noted that circRNA exhibits a higher resistance to degradation [21] and is often expressed in a cell type- and developmental stage-specific manner [17, 22]. With respect to the field of animal reproduction, circRNA expression have been well characterized in different types of tissues and cells, including ovary [18, 23, 24], testis [18, 25, 26], placenta [27], follicle [19, 28], spermatogenic cell [29], granulosa cell [30, 31], embryonic stem cell (ESC) [32], induced pluripotent stem cell (iPS) [33], germline stem cell [34], oocyte and embryo [17, 22, 35]. However, only two circRNAs in the reproduction field, namely *circBIRC6* and *circCORO1C*, have so far functionally been proved to be involved in the regulation of maintenance of ESC pluripotency and somatic cell reprogramming [32]. Although the expression of circRNAs in porcine multiple tissues has been reported [18, 36], its expression and function in porcine oocyte meiotic maturation remain unclear.

Here, we address the expression and function of circRNA in porcine oocyte meiotic maturation. Particularly, we identified thousands of circRNAs in both cumulus cells and oocytes, some of which often display a developmental stage-specific expression. Unexpectedly, we found that maternally expressed *circARMC4* is an essential regulator for oocyte meiotic maturation and development. Therefore, our findings could have important implications in selecting potential biomarkers in cumulus cells to predict oocyte meiotic and developmental competence and developing strategies that improve assisted reproductive techniques in humans.

RESULTS

Characterization of circRNAs expressed in porcine cumulus cells and oocytes during meiotic maturation

Since only the very limited amount of total RNA from thousands of porcine oocytes can be obtained, it is insufficient to meet the minimal needs of deep circRNA sequencing. To overcome the technical challenge, a mathematical method, named “complementary set

function”, was applied to screen circRNAs expressed in oocytes during meiotic maturation. Thus, COCs and pure cumulus cells termed as GCC at GV stage, mixture samples of oocytes with first polar body extrusion and cumulus cells, and pure cumulus cells termed as MCC, were separately sequenced on the Illumina HiSeq platform (Figure 1A). We then identified specific circRNAs expressed in oocytes by comparing circRNA transcripts of pure cumulus cells and mixture samples of cumulus cells and oocytes before and after maturation (Figure 1A). To verify the reproducibility of sequencing data, we collected three sets of each sample. The correlation coefficient between two biological replicates ranged from 0.813 to 1, suggesting reliable sequencing data. A total of 803 million valid reads were obtained by removing the adapter and low-quality sequences and were mapped to the porcine reference genome (Supplementary Table 2). We totally identified 7,224 circRNAs from 3,419 host genes, including 7,067 circRNAs from 3,329 host genes in cumulus cells and 637 circRNAs from 476 host genes in oocytes, respectively (Supplementary Table 3). The majority of host genes produce a single circRNA, whereas a few host genes generate multiple different circRNA species, specifically, 45.36% of host genes (1,510/3,329) in cumulus cells and 19.12% (91/476) in oocytes (Supplementary Table 4). The analysis of host gene distribution on chromosome revealed that circRNAs are widely transcribed from 18 autosomes and the X chromosome (Figure 1B). Furthermore, chromosome 1 produces the most circRNAs in both cumulus cells and oocytes, whereas the least circRNAs are separately generated on chromosome 17 in cumulus cells and chromosome 12 in oocytes (Figure 1B). The analysis of circRNA distribution in the genome indicated that most circRNAs is produced from exonic (60.82% in cumulus cell vs. 53.67% in oocyte) and intronic regions (28.45% vs. 32.99%), while a small fraction of circRNAs originate from intergenic regions (10.73% vs. 13.34%) (Figure 1C). The average GC content of circRNA is around 47% in cumulus cells and is approximately 45% in oocytes, which are similar to those of linear mRNA molecules in pigs (Figure 1D). Collectively, we identify and characterize thousands of circRNAs that are separately expressed in porcine cumulus cells and oocytes during meiotic maturation.

Identification and validation of differentially expressed circRNAs in both cumulus cells and oocytes

To evaluate dynamic changes of circRNA expression in both cumulus cells and oocytes during meiotic maturation, valid reads in RNA-sequencing data were quantified before and after oocyte maturation. Among all circRNAs detected in cumulus cells, 77 circRNAs and

418 circRNAs are specifically expressed in GCC and MCC, respectively, whereas 6,572 circRNAs are commonly expressed in cumulus cells between the two stages (Figure 2A). Meanwhile, of all circRNAs identified in oocytes, 428 circRNAs and 80 circRNAs are exclusively expressed in GV oocyte and MII oocyte, respectively, whereas 129 circRNAs are co-expressed in oocytes between the two stages (Figure 2A). In a comparison of MCC and GCC, the 928 host genes produce 1,902 differentially expressed circRNAs (DECs) (Supplementary Table 5) ($P < 0.05$), including 1,602 upregulated and 300 downregulated (Figure 2B), while

191 circRNAs (9 upregulated and 182 downregulated) from 30 host genes are differentially expressed between MII oocyte and GV oocyte (Figure 2B, Supplementary Table 5) ($P < 0.05$). Next, we performed hierarchical clustering analysis of the top 100 differentially expressed circRNAs in both cumulus cells and oocytes. As shown in the heatmap, samples at the same stages are clustered together, and the expression levels of circRNAs exhibit dynamic changes during oocyte maturation (Figure 2C). To validate the circRNA sequencing data, the expression levels of 10 circRNAs (5 top upregulated in cumulus cells and 5 top downregulated in oocytes) before and

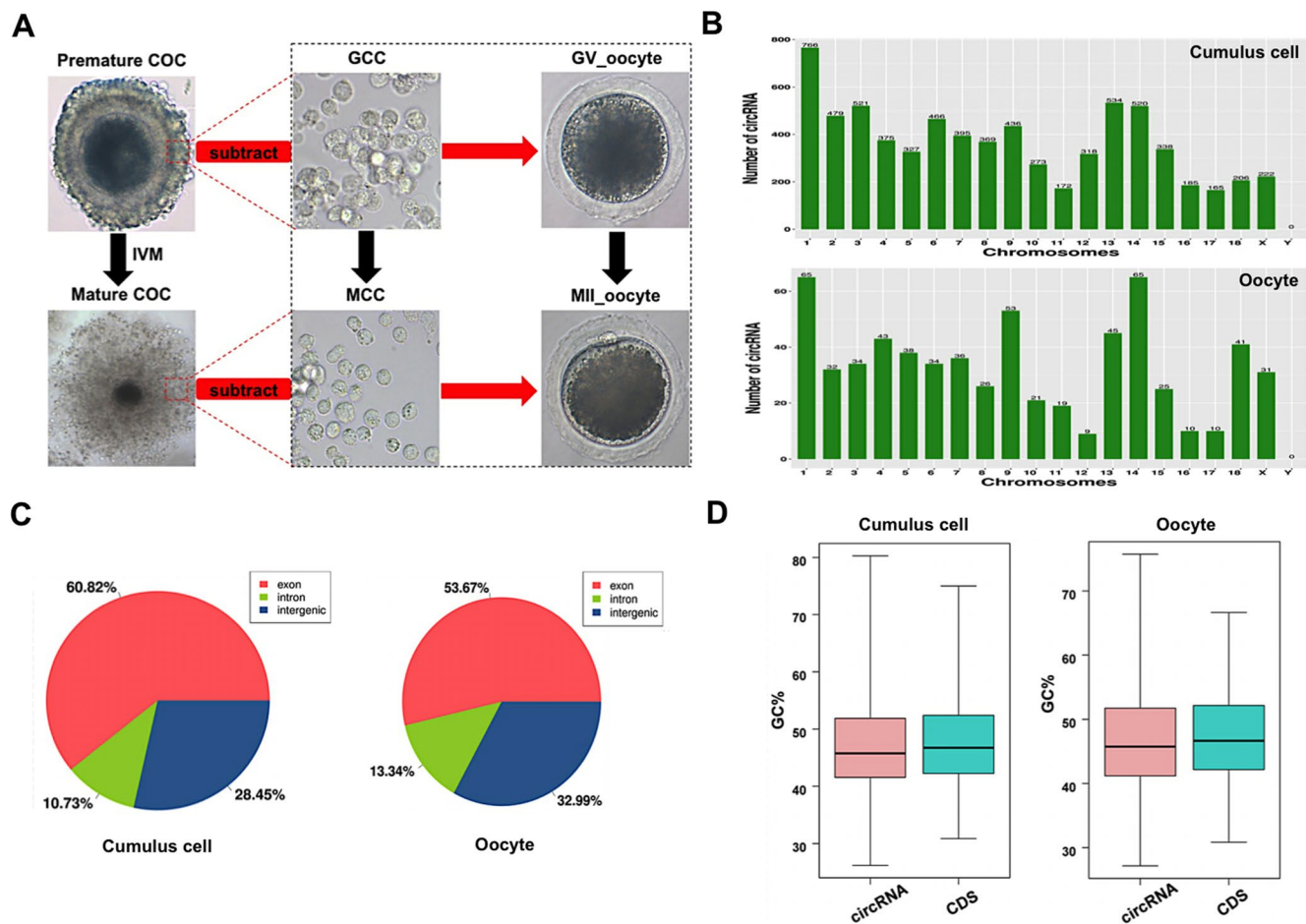


Figure 1. Characteristics of circRNAs expressed in porcine cumulus cells and oocytes. (A) Schematic illustration of experimental designs identifying circRNAs expressed in cumulus cells or oocytes before and after maturation. Premature COCs, cumulus cells before maturation (termed GCC), mature COCs, and cumulus cells after maturation (termed MCC) were collected respectively for RNA-seq. Of note, circRNAs expressed in the GCC were subtracted from these identical circRNAs expressed in the premature COCs to identify circRNAs expressed in GV oocytes, which are termed GV oocyte. Similarly, circRNAs expressed in MCC were subtracted from these identical circRNAs expressed in the mature COCs to identify circRNAs expressed in MII oocytes, which are termed MII oocyte. COCs, cumulus-oocyte complexes; GV, germinal vesicle; MII, metaphase II; IVM, in vitro maturation. Red dashed insets show cumulus cells before and after oocyte maturation at high magnification. (B) Chromosome distribution of circRNAs. Chromosome distribution of total circRNAs expressed in cumulus cells or oocytes was shown in the upper panel and bottom panel, respectively. (C) Genomic location of circRNAs. Genomic distribution of total circRNAs expressed in cumulus cells or oocytes was shown in the left panel and right panel, respectively. (D) GC enrichment of circRNAs and mRNAs. GC content of total circRNAs and mRNAs expressed in cumulus cells or oocytes was separately shown in the left panel and right panel.

after maturation, namely *circCORO1C*, *circVCAN*, *circLAPTM4B*, *circANXA2*, *circSCARB1* and *circZP4*, *circPRKCH*, *circCHL1*, *circVOCH1*, *circESRP1*, were analyzed by quantitative real-time PCR. These 10 circRNA candidates are first shown to be resistant to RNase R treatment, which verified their circularized characteristics (Supplementary Figure 2A–2D). The expression patterns of these selected circRNAs during oocyte maturation are highly consistent with the trends obtained from circRNA sequencing data (Figure 2D), confirming the results obtained by circRNA sequencing. Together, a fraction of circRNAs identified in both cumulus cells and oocytes exhibit stage-dependent dynamic expressions during meiotic maturation.

Functional analysis of host genes of differentially expressed circRNAs in both cumulus cells and oocytes

Under the assumption that circRNA functions may be relevant to the known functions of host genes, we performed GO and KEGG pathway analysis of the host genes producing DECs to predict their potential functions during oocyte maturation. The host genes generating DECs in both cumulus cells and oocytes were classified into three main categories (biological process, cellular component, and molecular function) according to the GO database. The 928 host genes producing DECs in cumulus cells are totally enriched in 4,092 GO terms, among these, 146 GO terms are significantly enriched in three GO functions or undetermined function ($P < 0.05$), namely, 73 under “biological process”, 31 under “cellular component”, 41 under “molecular function” and 1 under “undetermined function” (Supplementary Table 6). The top-ranking 25 biological processes, 15 cellular components, 10 molecular functions, and host genes involved in each GO term were listed (Figure 3A, Supplementary Table 6), such as intracellular signal transduction (48 genes, e.g. *ADCY3*, *AKT3*, and *CDC42BPA*), negative regulation of cytoplasmic translation (4 genes, namely, *CPEB1*, *CPEB2*, *CPEB3*, and *CPEB4*), signal transduction by protein phosphorylation (12 genes, e.g. *BMPRI1B*, *MAP3K2*, and *TGFBRI*), regulation of GTPase activity (14 genes, e.g. *ARHGAP6*, *PRKG1*, and *RICTOR*), cell-cell junction (19 genes, e.g. *ACTR3*, *AFDN*, and *CASK*). On the other hand, the 30 host genes producing DECs in oocytes are totally enriched in 865 GO terms, of these, 236 GO terms are significantly enriched in three GO functions or undetermined function (Supplementary Table 6) ($P < 0.05$). The most significant biological processes, cellular components and molecular functions, and host genes involved in each GO term were listed (Figure 3B, Supplementary Table 6) ($P < 0.05$), such as female meiotic division (2 genes, namely, *SYCP2* and *WEE2*), G-protein coupled receptor activity (3 genes, e.g.

CALCR, *GABBR1*, and *SENP7*). In addition, the KEGG analysis of host genes producing DECs in cumulus cells displayed 28 significant pathways (Figure 3C, Supplementary Table 7) ($P < 0.05$), including progesterone-mediated oocyte maturation (16 genes), oocyte meiosis (17 genes), tight junction (17 genes), FoxO signaling (16 genes), MAPK signaling (21 genes), TGF- β signaling (10 genes), Wnt signaling (16 genes), Hippo signaling (14 genes). At the same time, we also found that the host genes generating DECs in oocytes are enriched in 30 significant pathways (Figure 3D, Supplementary Table 7) ($P < 0.05$), such as cAMP signaling (6 genes), cGMP-PKG signaling (5 genes), VEGF signaling (3 genes). Overall, the host genes-enriched aforementioned pathways in both cumulus cells and oocytes are mainly related to intercellular crosstalk between two cell types, or oocyte itself maturation. Therefore, these results indicated that DECs generated in both cumulus cells and oocytes probably exert critical functions in porcine oocyte maturation.

Prediction of miRNA targets potentially sponged by circRNAs expressed in both cumulus cells and oocytes

It is previously reported that circRNA can sponge miRNAs to indirectly regulate gene expression in a post-transcriptional manner [37]. To assess whether all circRNAs identified in both cumulus cells and oocytes function as miRNA sponge, we predicted miRNA targets of these circRNAs using bioinformatic tools. We found that 7,165 out of 7,224 circRNAs (99.18%) have miRNA binding sites, whereas a very few circRNAs are predicted to have no potential miRNA targets. Furthermore, 411 putative microRNA targets on 7,165 circRNAs were commonly predicted using Targetscan and miRanda (Figure 4A). Each circRNA may bind to one or multiple miRNA targets. Thus, the proportion of circRNA containing different numbers of miRNA targets is further measured in our study. Most circRNAs have at least two miRNA binding sites, of which the proportion of circRNA containing 6–10 miRNA targets is the highest one (Figure 4B). Subsequently, we found 411 and 373 putative miRNA targets for 1,897 out of 1,902 DECs in cumulus cells and 180 out of 191 DECs in oocytes, respectively. The interaction relationships between selected representative DECs in both cumulus cells and oocytes and their predicted miRNA targets are shown (Figure 4C, 4D). These data revealed that most DECs in the two cell types indeed contain multiple miRNA targets. It is noted that some miRNAs sponged by circRNAs have been shown to control cumulus cell function, oocyte maturation, and early embryo development. For example, miRNA-224 targeted by *circRNA3798* in cumulus cells [10], miRNA-21 bound by *circRNA193* [11], and miRNA-378 bound by

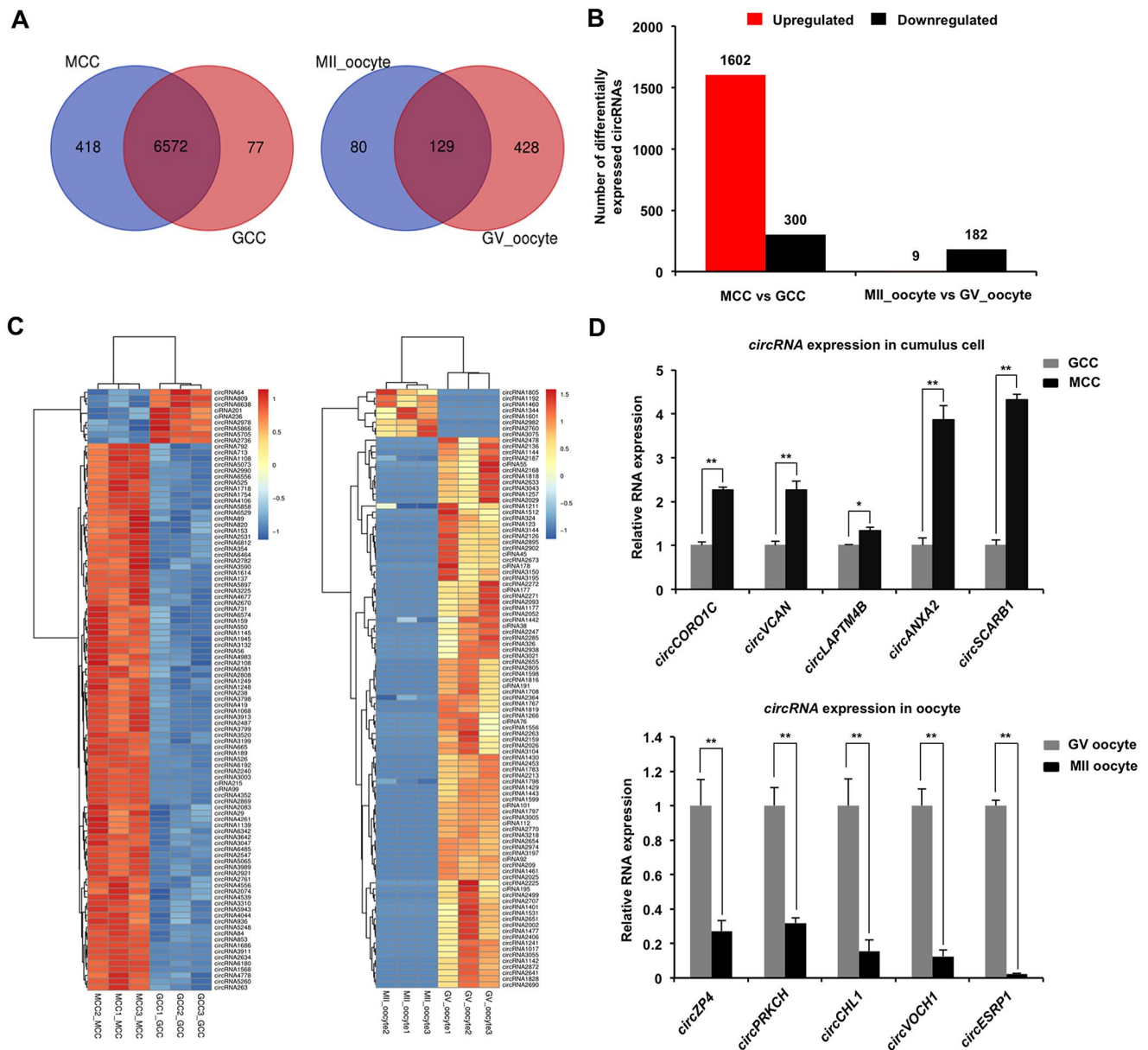


Figure 2. Identification and validation of differentially expressed circRNAs (DECs) in both cumulus cells and oocytes during meiotic maturation. (A) Venn diagram of circRNAs identified in cumulus cells or oocytes. Cumulus cells and oocytes before and after meiotic maturation were pooled for RNA-seq. Expression levels of circRNAs in cumulus cells (left panel) and oocytes (right panel) were analyzed by means of a binominal statistical test. Overlapping circles present circRNAs that are common for cumulus cells or oocytes between two different stages. Non-overlapping circles indicate circRNAs that are specific for cumulus cells or oocytes before (pink) and after (blue) meiotic maturation. (B) The number of differentially expressed circRNAs in cumulus cells or oocytes before and after meiotic maturation. The results were considered statistically significant at $P_{adjusted} < 0.05$ and \log_2 fold change ≥ 1 . Red bars indicate up-regulated circRNAs; black bars denote down-regulated circRNAs. (C) Heatmap illustrating the expression patterns of differentially expressed circRNAs in cumulus cells (left panel) or oocytes (right panel) before and after meiotic maturation. The red blocks represent up-regulated circRNAs, and the blue blocks represent down-regulated circRNAs. The color scale of the heatmap indicates the expression level, where the brightest blue stands for $-1.0 \log_2$ fold change and the brightest red stands for 1.0 or $1.5 \log_2$ fold change. (D) Validation of the selected differentially expressed circRNAs identified in both cumulus cells and oocytes. The several selected circRNAs were chosen from top up and top down-regulated circRNAs in cumulus cells or oocytes. Relative abundance of circRNAs in cumulus cells (upper panel) and oocytes (bottom panel) was determined by qPCR. The data were normalized against endogenous housekeeping gene *EF1 α 1*, and the value for cumulus cells or oocytes at GV stage was set as one. The data are shown as mean \pm S.E.M. Statistical analysis was performed using *t*-student test. Values with asterisks vary significantly, * $P < 0.05$, ** $P < 0.01$.

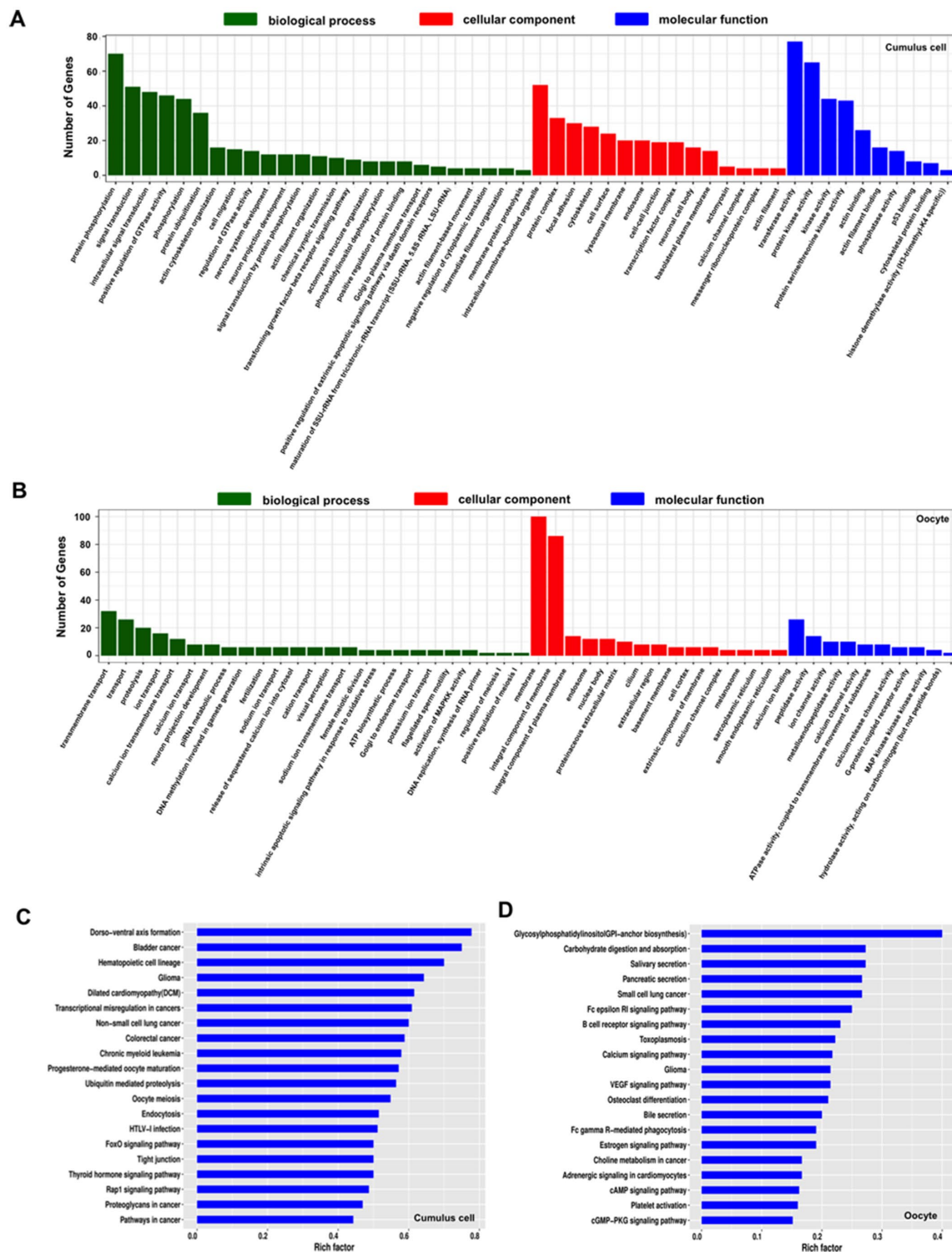


Figure 3. GO and KEGG analysis of host genes of differentially expressed circRNAs (DECs) in both cumulus cells and oocytes during meiotic maturation. (A) GO analysis of the top enriched terms of the differentially expressed circRNA hosting genes identified in cumulus cells. Host genes of differentially expressed circRNAs were classified into three categories of the GO classification (blue bars: biological processes, green bars: cellular components and orange bars: molecular functions). **(B)** KEGG analysis of the top enriched signaling pathways of the differentially expressed circRNA hosting genes identified in cumulus cells. **(C)** GO analysis of the top enriched terms of the differentially expressed circRNA hosting genes identified in oocytes. Host genes of differentially expressed circRNAs were classified into three categories of the GO classification (blue bars: biological processes, green bars: cellular components and orange bars: molecular functions). **(D)** KEGG analysis of the top enriched signaling pathways of the differentially expressed circRNA hosting genes identified in oocytes.

circRNA2982 [38] in oocytes. Altogether, these results demonstrate that circRNAs identified in both porcine cumulus cells and oocytes could have potential miRNA binding sites.

***CircARMC4* knockdown impairs porcine oocyte meiotic maturation and chromosome alignment**

To further determine whether circRNAs identified in porcine oocytes by RNA sequencing function in meiotic maturation, one top upregulated circRNA, namely, *circRNA2982* (also called as *circARMC4*) from the host gene *ARMC4*, was selected for functional research. Firstly, the relative abundance of *circARMC4* in oocytes before and after maturation was analyzed by qPCR. We found that the expression levels of *circARMC4* in MII

oocytes are significantly higher than those in GV oocytes (Figure 5A), which is consistent with the trend obtained from RNA sequencing data. Furthermore, *circARMC4* transcripts, but not its corresponding linear counterparts, are resistant to RNase R treatment, which confirmed its circularized feature (Supplementary Figure 2C, 2D). Sanger sequencing of qPCR products spanning back-splicing sites between exon 14 and exon 15 also verified that it is indeed real circRNA (Figure 5B). To examine the role of *circARMC4* in oocyte maturation, *circARMC4* was knocked down by microinjecting siRNA into GV oocytes. Results revealed that siRNA could significantly reduce the expression of *circARMC4*, but not its linear counterparts (Figure 5C, 5D). Phenotypically, we found that *circARMC4* knockdown could apparently reduce the rate of first polar body extrusion (67.27 ± 2.01 and

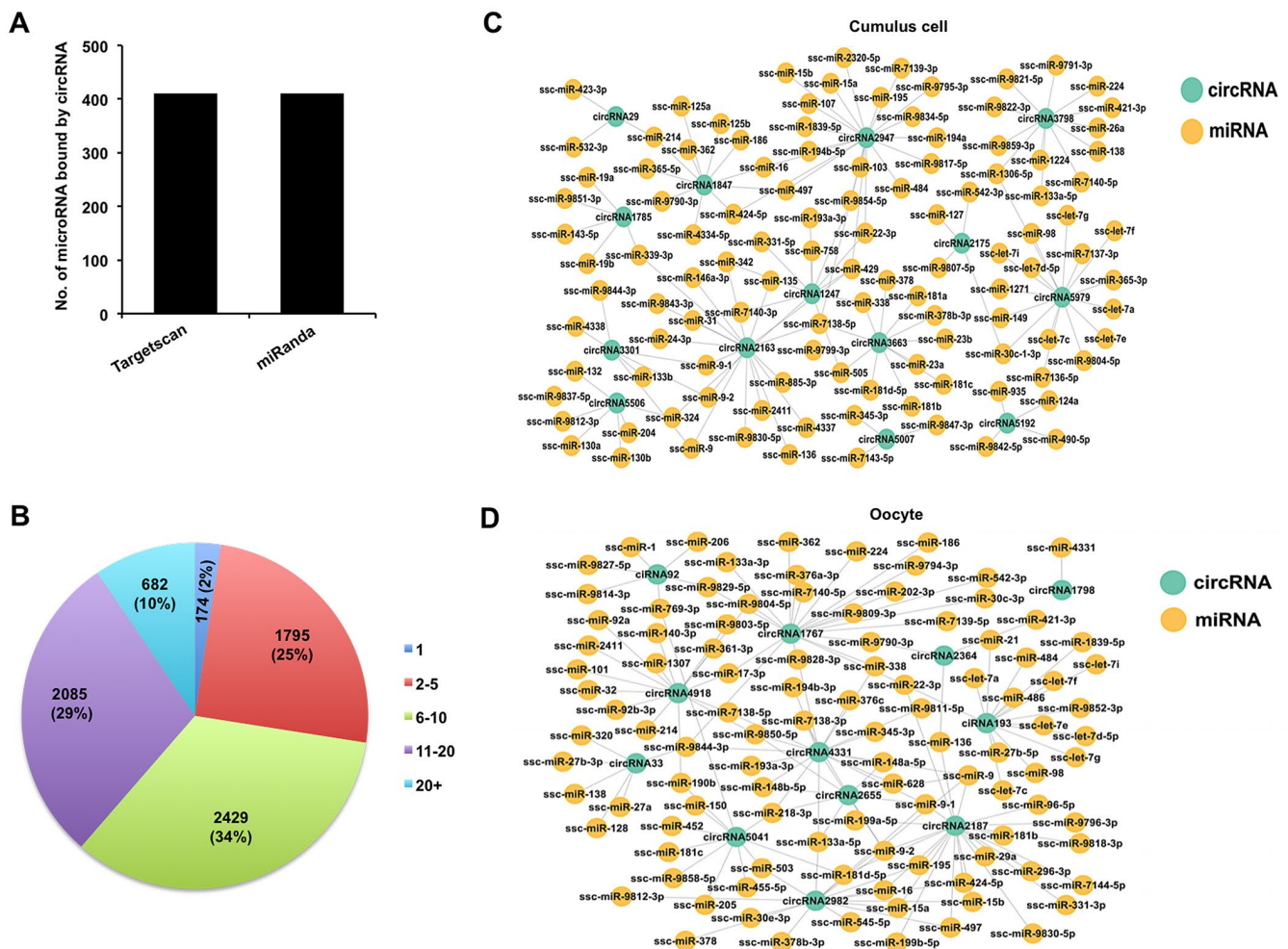


Figure 4. Analysis of interaction between DECs and miRNAs in both cumulus cells and oocytes. (A) Analysis of number of miRNAs for circRNAs by Targetscan and miRanda. **(B)** Analysis of the proportion of circRNA processing different numbers of miRNA targets. **(C)** Analysis for predicted targeted miRNAs of the selected DECs identified in cumulus cells. The selected circRNAs were chosen from top DECs in cumulus cells. Blue circles represent circRNA, and yellow circles represent miRNA. **(D)** Analysis for predicted targeted miRNAs of the selected DECs identified in oocytes. The selected circRNAs were chosen from top DECs in oocytes. Blue circles represent circRNA, and yellow circles represent miRNA.

69.04±5.51 vs. 40.77±3.49) (Figure 5E, 5F). Also, oocytes with first polar body in control groups display bipolar spindles and normal linear chromosome morphology, while chromosomes in the substantial fraction of *circARMC4* knocked down oocytes are misaligned at the metaphase plate even though the spindles are morphologically normal (Figure 5G). We further observed that the proportion of MII oocytes with abnormal chromosomes in the *circARMC4* knockdown group is significantly higher than that in control groups (36.25±2.60 and 39.49±0.89 vs. 58.51±4.10) (Figure 5H). In addition, knockdown of *circRICTOR* specifically expressed in cumulus cells also caused both the failure of cumulus expansion and the reduction in the rate of oocyte maturation and embryo development (Supplementary Figure 3). Therefore, these data document that maternally expressed *circARMC4* is essential for oocyte meiotic maturation in pigs.

***CircARMC4* knockdown reduces developmental competence of porcine early embryos**

Given that developmental competence of embryos largely depends on oocyte quality [1], we thus attempted to explore whether *circARMC4* knockdown in oocytes affects early development of porcine embryos. MII oocytes from both *circARMC4* knockdown group and two control groups were parthenogenetically activated and cultured up to the blastocyst stage. We found that *circARMC4* knockdown significantly reduced developmental efficiency of 2-cell (90.10±2.17 and 91.23±8.77 vs. 52.71±7.41), 4-cell (66.34±3.23 and 63.30±5.45 vs. 22.47±7.11), 8-cell embryos (54.72±1.59 and 57.79±2.73 vs. 7.41±7.40) and blastocysts (23.75±1.62 and 24.76±2.46 vs. 7.41±7.40) (Figure 6A, 6B), suggesting that *circARMC4* knockdown could impair the developmental competence of oocytes. Hence, these results indicate that *circARMC4* knocked down oocytes possess poor developmental competence.

DISCUSSION

Although the expression profiles of circRNAs in different porcine tissues have been well studied [18, 36], its expression and function in porcine oocyte meiotic maturation are yet to be characterized. We here identified thousands of circRNAs expressed in both cumulus cells and oocytes by deep RNA sequencing, some of which show spatio-temporal specific differential expression during meiotic maturation. Functional annotations of these DECs revealed that they could be engaged in the regulation of oocyte meiotic maturation through sponging microRNAs. Importantly, we further showed that *circARMC4*, a top up-regulated circRNA in oocytes, is required for porcine oocyte meiotic maturation and early embryo development. Therefore, these results indicate

that circRNAs expressed in both cumulus cells and oocytes could play a critical role in porcine oocyte meiotic maturation and early embryo development.

In this study, we detected 7,067 circRNAs in cumulus cells and 637 circRNAs in oocytes, respectively, indicating that cell type-dependent characteristics of circRNA expression and differential regulation of circularization events in different cells. A similar phenomenon is also observed in other studies [18, 39]. In addition, it is evident that cumulus cells are transcriptionally high active in the process of oocyte maturation while oocyte always retains in a transcriptionally quiescent state [40]. Cumulus cells could produce much more transcripts relative to the stored maternal transcripts in oocytes, and circRNA biogenesis mainly depends on the back-splicing of pre-mRNA transcribed in a cell [16]. We thus speculated that a larger amount of circRNAs produced in cumulus cells could be attributed to its higher transcriptional activity. Interestingly, we noted that the number of circRNAs identified in cumulus cells or oocytes apparently differs from that found in other species, such as cattle [8], *Xenopus* [35], mice [17] and humans [22], suggesting that circRNA expression may have a feature of species diversity. In addition, the number of circRNAs originated from each chromosome in both cumulus cells and oocytes also varies, which may be associated with the chromosome length. Regarding the origin of circRNAs in both cumulus cells and oocytes, it was shown that circRNAs mainly originate from exons, which is consistent with the previous studies [18]. Furthermore, consistent with data reported in other porcine cell types [18], the GC content of circRNA in both cumulus cells and oocytes is similar to that of linear mRNA molecules, implying that thermal stability of circRNA could be conserved across different cell types. Previous studies have revealed that circRNAs exhibit tissue- and developmental stage-specific expression in pigs [18], mice [17] and humans [22]. Likewise, we also found that circRNAs are expressed in a stage-specific manner during oocyte maturation. Based on the above analysis, it is concluded that circRNAs identified in our study harbor some unique or common features between different cell types or species.

Potential functions of circRNAs in porcine cumulus cells and oocytes can be indirectly predicted by analyzing their host genes. GO and KEGG analysis of host genes producing DECs in cumulus cells revealed that GO terms are mainly enriched in the signal transduction related biological processes and pathways, such as regulation of GTPase activity and tight junction. The GTPase signaling pathway is reported to play critical roles in a wide range of cellular processes [41]. Previous studies indicated the activation of GTPases is responsible for the accumulation

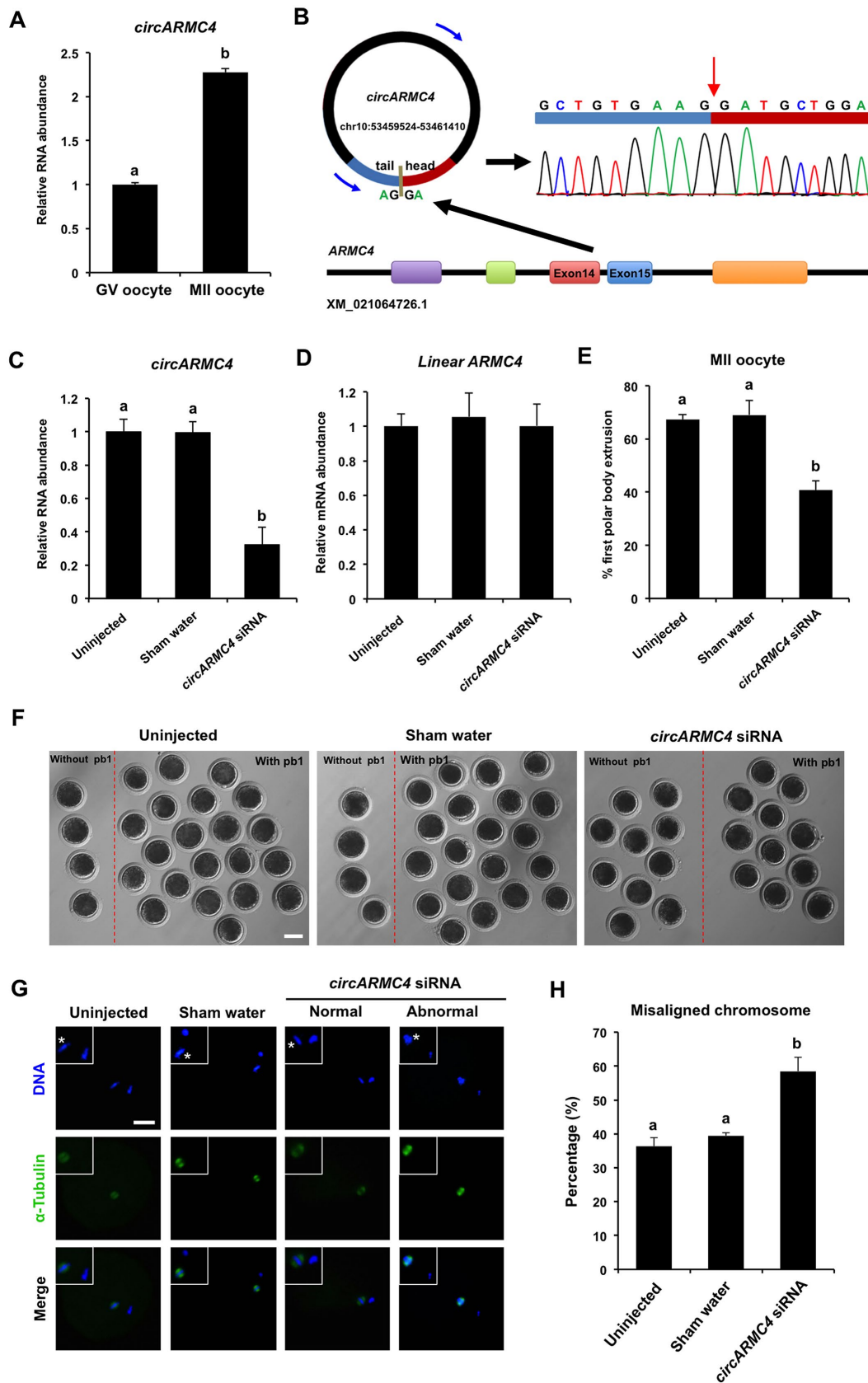


Figure 5. Effect of *circARMC4* knockdown on oocyte meiotic maturation and chromosome alignment. (A) *CircARMC4* expression in both GV oocytes and MII oocytes. Relative expression of *circARMC4* was determined by qPCR. The data are analyzed using student's *t* test and are shown as mean \pm S.E.M. Different letters on the bars indicate significant differences ($P < 0.05$). (B) Schematic

illustration showed the ARMC4 exon 14 and exon 15 circularization forming circARMC4 (blue arrow). The presence of *circARMC4* was validated by qPCR, followed by Sanger sequencing. Red arrow represents “head-to-tail” *circARMC4* splicing sites. The expression levels of *circARMC4* (C) and linear *ARMC4* (D) in the MII oocytes derived from GV oocytes. GV oocytes were injected with *circARMC4* siRNA, followed by maturation *in vitro* for 44 h. Oocytes injected with water and uninjected oocytes were served as a sham control and a blank control, respectively. One hundred matured oocytes were collected for qPCR analysis. Relative abundance of *circARMC4* and linear *ARMC4* was determined by qPCR from four independent replicates. The data were normalized against endogenous housekeeping gene *EF1α1* and the value for the blank control was set as one. The data are shown as mean ± S.E.M. One-way ANOVA was used to analyze the data and different letters on the bars indicate significant differences ($P < 0.05$). (E) Analysis of the rate of oocyte maturation. The number of oocytes with first polar body after *in vitro* maturation for 44 h was recorded and the rate of first polar body extrusion was statistically analyzed by one-way ANOVA. The experiment was repeated four times with at least 100 oocytes per group. The data are shown as mean ± S.E.M and different letters on the bars indicate significant differences ($P < 0.05$). (F) Representative images of oocytes after *in vitro* maturation. The oocytes without pb1 and the oocytes with pb1 were shown in both the left side and the right side of each image, respectively. Scale bar: 100 μm. (G) Spindle and chromosome morphology in MII oocytes. Matured oocytes were stained for α-tubulin (green) and DAPI (blue). Shown are representative images obtained using confocal laser-scanning microscopy. The experiment was independently repeated three times with at least 40 oocytes per group. Bottom panel in each group shows the merged images between α-tubulin and DNA. White square insets indicate both spindles and chromosomes at a more focused view. Asterisks indicate chromosomes. Scale bar: 50 μm. (H) Analysis of the percentage of oocytes with abnormal chromosome morphology. The chromosome morphology of MII oocytes was scored according to a published method. The data were statistically analyzed by one-way ANOVA. The data are shown as mean ± S.E.M and different superscripts on the bars indicate significant differences ($P < 0.05$).

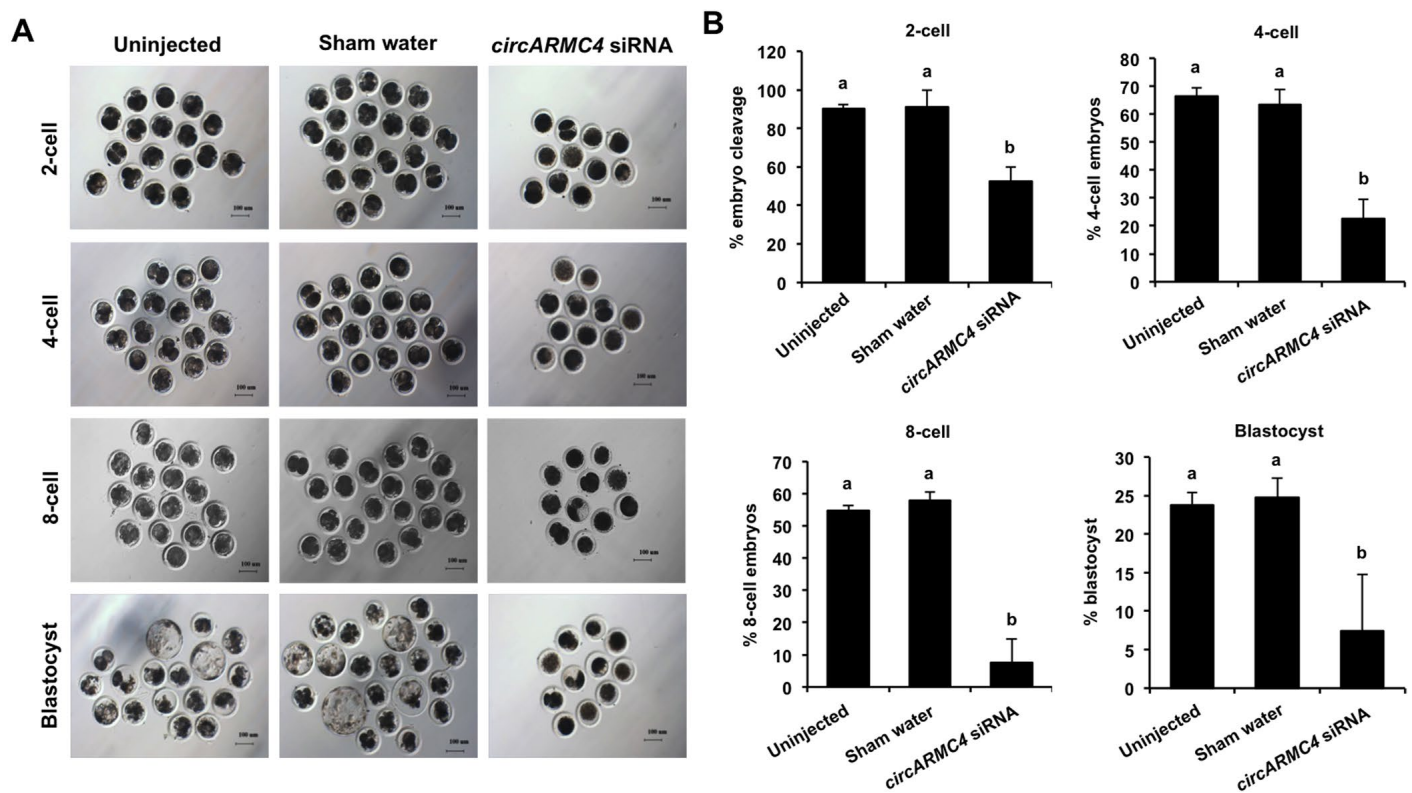


Figure 6. Effect of *circARMC4* knockdown on developmental competence of porcine early embryos. (A) Representative brightfield images of embryos at different developmental stages. GV oocytes were injected with siRNA or water and GV oocytes without any treatment, followed by maturation *in vitro* for 44 h. Oocytes with first polar body were parthenogenetically activated (n=51, 57, 28) and cultured up to the blastocyst stage. The brightfield images of 2-cell, 4-cell, 8-cell embryo and blastocyst were captured by epifluorescence microscopy. Scale bar: 100 μm. (B) Analysis of the developmental rate of embryos at different developmental stages. The number of embryos at different developmental stages was recorded (2-cell: n=46, 52, 14; 4-cell: n=34, 38, 6; 8-cell: n=28, 33, 2; blastocyst: n=12, 14, 2) and the corresponding data were statistically analyzed by one-way ANOVA. All experiment was repeated three times. The data are shown as mean ± S.E.M and different letters on the bars indicate significant differences ($P < 0.05$).

of cell junction proteins to regulate the establishment of cell junctions and cell-cell adhesion between oocytes and cumulus cells [42, 43]. Tight junction is shown to regulate the transport of macromolecules from granulosa cells to oocytes in chicken [44]. Based on these studies and our results, it is plausible that DECs identified in cumulus cells may be engaged in the intercellular communications between porcine oocytes and cumulus cells. Moreover, other signaling pathways related to animal reproduction, eg. Progesterone-mediated oocyte maturation, FoxO signaling, and MAPK signaling, are also significantly enriched. Particularly, small GTPase RhoA [45], MAPK signaling members [46] are essential for porcine oocyte maturation. On the other hand, GO terms significantly enriched by host genes generating DECs in oocytes are mainly related to oocyte meiosis, such as female meiotic division, cAMP signaling, and VEGF signaling. For instance, both WEE2 enriched in the female meiotic division and cAMP molecules have been shown to inhibit the resumption of oocyte meiosis in several species [47, 48]. In contrast, VEGF supplement significantly improved maturation rate of oocytes in cattle [49], sheep [50] and pigs [51]. Altogether, we thus reasoned that DECs identified in oocytes could positively or negatively regulate porcine oocyte meiotic maturation in a synergistic manner.

It has been shown that exon-derived circRNAs preferentially function in the post-transcriptional regulation [20]. Similarly, we found that the vast majority of DECs identified in this study have putative miRNA binding site, which indicates that most DECs probably act as miRNA sponge. CircRNA-miRNA network analysis further revealed that DECs in the analyzed samples can interact with miRNA at multiple direction levels, which is consistent with that observed in the previous studies [18, 19]. This potential interplay between circRNA and miRNA could provide a reference for elucidating regulatory mechanisms of these DECs in oocyte meiotic maturation. Indeed, recent studies have shown that maternal miRNA participates in regulating oocyte maturation and early embryo development in several species, including pigs [11], medaka [12], and *C. elegans* [13]. Specifically, miRNA-7 was found to inhibit epidermal growth factor receptor (EGFR) expression in human cancer cells [52] and EGFR signaling is required for cumulus cell expansion and oocyte maturation [53], suggesting that miRNA-7 may negatively regulate oocyte maturation. Our results indicated that these above-mentioned miRNAs could be bound by DECs expressed in both cumulus cells and oocytes. Therefore, these DECs may block the functional roles of miRNAs by sequestering them, thereby regulating porcine oocyte maturation and early embryo development.

Examining the direct roles of individual circRNAs in oocyte meiotic maturation and embryo development should be subject in future investigations. In the current study, a maternally expressed *circARMC4* was selected to explore its roles in porcine oocyte maturation. We discovered that *circARMC4* knockdown led to a significant reduction in the rate of oocyte maturation and early embryo development and a higher proportion of misaligned chromosome. To our knowledge, this is proved for the first time that circRNA is essential for oocyte maturation and early embryo development. It is previously reported that Gudu is the *Drosophila* homolog of mammalian *ARMC4* that is the host gene of *circARMC4* and has been shown to be required for spermatogenesis, but not female fertility [54], predicting that *circARMC4* could be involved in the regulation of mammalian reproduction. Of note, circRNA can also execute roles in other models of post-transcriptional regulation. We cannot thus exclude the possibility that *circARMC4* might exert functions in porcine oocyte maturation and early embryo development via other mechanisms, such as RNA binding protein sponge, mRNA trap and circRNA itself translation. These hypotheses, however, need to be further established by additional experimental designs in future studies.

In conclusion, these results demonstrate that cumulus cells and oocytes generate abundant circRNAs during meiotic maturation, of which thousands of circRNAs are expressed in a developmental stage-specific manner. Our data also document for the first time that maternally expressed *circARMC4* is essential for porcine oocyte meiotic maturation and early embryo development.

MATERIALS AND METHODS

Ethics statement

All experiments using pigs were carried out according to the guidelines of the Institutional Animal Care and Use Committee (IACUC) at Anhui Agricultural University.

In vitro maturation of oocytes

Ovaries were collected from a local slaughterhouse and transported to the laboratory at 28-35 °C in physiological saline solution. Follicular fluids from antral follicles of different diameters at 1-2 mm, 3-6 mm, and more than 6 mm were aspirated using a sterile 10 ml syringe with 18 gauge needles. Cumulus-oocyte complexes (COCs) from each type of follicles were then selected under a stereomicroscope. Subsequently, appropriately 50 COCs were transferred to 400 µl *in vitro* maturation medium (TCM-199 supplemented with 5% FBS, 10% porcine follicular fluid, 10 IU/ml eCG, 5 IU/ml hCG, 100 ng/ml L-Cysteine, 10 ng/ml EGF, 100 U/ml penicillin and 100

mg/ml streptomycin) covered with mineral oil in 4-well plate and cultured for 44 h at 38.5 °C, 5% CO₂, 95% air and 100% humidity. Cumulus cells surrounding oocyte were removed by gentle pipetting in 1 mg/ml hyaluronidase solution. The normal nuclear maturation of oocytes was indicated by first polar body (pb1) extrusion.

Collection of RNA sequencing samples

Four types of sample were collected to meet the minimum amount of total RNA for RNA sequencing. First, the mixed cells consisting of fully-grown GV oocytes and cumulus cells were collected. Second, cumulus cells isolated from fully-grown cumulus-oocyte complexes were solely collected and were also termed GCC. Third, after meiotic maturation of oocytes, the mixed cells containing MII oocytes and its surrounding cumulus cells were collected. Fourth, cumulus cells encircling MII oocyte were only collected and were also termed MCC.

circRNA library construction and sequencing

Total RNA was isolated and purified using Trizol reagent (Invitrogen, Carlsbad, CA, USA) following the manufacturer's procedure. The RNA amount and purity of each sample was quantified using NanoDrop ND-1000 (Wilmington, DE, USA). The RNA integrity was assessed by Agilent 2100 with RIN number >7.0. Approximately 5 ug of total RNA was used to deplete ribosomal RNA according to the manuscript of the Ribo-Zero™ rRNA Removal Kit (Illumina, San Diego, USA). After removing ribosomal RNAs, the left RNAs were fragmented into small pieces using divalent cations under high temperature. Then the cleaved RNA fragments were reverse-transcribed to create the cDNA, which was next used to synthesize U-labeled second-stranded DNAs with E. coli DNA polymerase I, RNase H and dUTP. An A-base is then added to the blunt ends of each strand, preparing them for ligation to the indexed adapters. Each adapter contains a T-base overhang for ligating the adapter to the A-tailed fragmented DNA. Single-or dual-index adapters are ligated to the fragments, and size selection was performed with AMPureXP beads. After the heat-labile UDG enzyme treatment of the U-labeled second-stranded DNAs, the ligated products are amplified with PCR by the following conditions: initial denaturation at 95 °C for 3 min; 8 cycles of denaturation at 98 °C for 15 sec, annealing at 60 °C for 15 sec, and extension at 72 °C for 30 sec; and the final extension at 72 °C for 5 min. The average insert size for the final cDNA library was 300 bp (±50 bp). At last, we performed the paired-end sequencing on an Illumina HiSeq 4000 (LC Bio, China) following the vendor's recommended protocol.

Bioinformatic analysis of circRNA

Firstly, Cutadapt was used to remove the reads that contained adaptor contamination, low quality bases and undetermined bases. Then sequence quality was verified using FastQC. We used Bowtie2 and Tophat2 to map reads to the genome of *Sus scrofa* (Ensemble database). Remaining reads (unmapped reads) were still mapped to the genome using Tophat-fusion. CIRCEXplorer was used to de novo assemble the mapped reads to circular RNAs at first; Then, back splicing reads were identified in unmapped reads by tophat-fusion and CIRCEXplorer. All samples were generated unique circular RNAs. The differentially expressed circRNAs were selected with log₂ (fold change) > 1 or log₂ (fold change) < -1 and with statistical significance (p value < 0.05) by t-test.

To analyze functions of differentially expressed circRNAs and their host genes of circRNAs involvement in the common biological processes, we selected host genes of different circRNAs for Gene Ontology (GO) analysis and Kyoto Encyclopedia of Genes and Genomes (KEGG) analysis. The circRNAs were classified into three categories of the GO database: biological processes, cellular components and molecular functions. KEGG database was used to ascribe identified circRNAs to particular biological mechanisms and cellular pathways. (the established criteria: p adjusted < 0.05). GO and KEGG enrichment analysis was performed using (<http://geneontology.org> and <http://www.kegg.jp/kegg>).

Microinjection

Three *circARMC4* siRNA species were designed to target different sites of porcine *circARMC4* sequence (GenePharma, Shanghai, China). All siRNA sequences used in the present study are shown in Supplementary Table 1. Microinjection was performed in T2 (TCM199 with 2% FBS) medium with 7.5 µg/ml CB on the heating stage of an inverted microscope (Olympus, Japan). Approximately 10 pl siRNA solution (20 µM) was microinjected into the cytoplasm of denuded GV oocytes. Two control groups (uninjected and RNase free water injection) were designed to exclude potential interferences of the microinjection technique. Oocytes from three groups were then matured *in vitro* for 44 h.

Lentivirus transduction of COCs

10 COCs were cultured in 40 µl droplet of IVM medium. Equal volumes of concentrated Lenti-green fluorescent protein (GFP) or Lenti-circRCTOR virus were added to each droplet to dilute the virus to the same concentration. Infected COCs were cultured in a humidified atmosphere of 95% air and 5% CO₂ at 38.5°C for 44 h.

Parthenogenetic activation

MII oocytes were stimulated with two pulses of direct current (1.56 kV/cm for 80 ms) by Cell Fusion Instrument (CF-150B, BLS, Hungary) in a chamber covered with activation medium (0.3 M mannitol supplemented with 0.1 mM CaCl₂, 0.1 mM MgCl₂ and 0.01% polyvinyl alcohol). Embryos were then incubated for 4 h in the chemically assisted activation medium (PZM-3 supplemented with 10 µg/ml cycloheximide and 10 µg/ml cytochalasin B). Next, embryos were cultured in fresh PZM-3 medium at 38.5 °C, 5% CO₂, and 95% air with saturated humidity.

Real-time quantitative PCR

Cumulus cells and oocytes were collected at GV and MII stage, respectively. Total RNA was extracted according to the manual of RNeasy Micro Kit (Qiagen) and was then incubated for 30 min at 37 °C with or without 5 U/µg of RNase R (Epicentre Biotechnologies). Reverse transcription was performed using a QuantiTect Reverse Transcription Kit (Qiagen, 205311) according to the manufacturer's instructions. Quantitative PCR was conducted using the SYBR Green PCR Master Mix (Roche, 04673514001) on a StepOne Plus Real-Time PCR System (Applied Biosystems). Reactions were carried out under the following conditions: 1 cycle of 95 °C for 2 min and 40 cycles of 95 °C for 5 s, 60 °C for 10 s. Analysis of gene expression employed relative quantification and 2^{-ΔΔCt} method. *EF1a1* was used as internal control. The PCR products were then run on 1.5 % agarose gels. The predicted strands were cut out directly for Sanger sequencing. Quantification of the fold change in gene expression was calculated using the comparative Ct (2^{-ΔΔCt}) method. All the primers used are shown in Supplementary Table 1. Three independent replicates were performed for each experiment.

Immunofluorescence staining

Oocytes were fixed with 4% paraformaldehyde (PFA) for 20 min. After washing three times, the fixed oocytes were permeabilized with 1% Triton X-100 in DPBS for 30 min at room temperature (RT) and then blocked with 2% BSA in DPBS at RT for 1 h. Oocytes were incubated in blocking buffer containing α-Tubulin antibody (Sigma, F2168, 1:200) overnight at 4°C. After washing 3 times with DPBS for 60 min. Finally, oocytes were counterstained for 10 min in 4, 6-diamidino-2-phenylindole dihydrochloride (DAPI) solution and loaded onto glass slides followed by being covered with a glass coverslip. Samples were imaged using confocal microscopy (Olympus, Tokyo, Japan). At least 10 oocytes per group were used for each experiment. The specificity of the α-

Tubulin antibody has been validated in Supplementary Figure 1.

Statistical analysis

All experiments were carried out at least three times. The data were analyzed using either Student's *t*-test or one-way ANOVA (SPSS 17.0) and were presented as mean ± standard error of mean (mean ± S.E.M). *P*<0.05 was considered to be statistically significant.

AUTHOR CONTRIBUTIONS

Conceived and designed the experiments: ZBC YHZ. Performed the experiments: DG TTX LZ XT YQW DDZ WN XQ YYM KYJ TY. Analyzed the data: ZBC DG YSL YHZ. Contributed reagents and materials: ZBC YHZ. Wrote the paper: ZBC YHZ.

ACKNOWLEDGMENTS

We thank MS. Lulu Song for her help in technical assistance.

CONFLICTS OF INTEREST

The authors declare no conflicts of interest with regard to the study.

FUNDING

This work was supported by grants from the Anhui Provincial Natural Science Foundation (1708085QC55 and 1908085MC97), the Science and Technology Major Project of Anhui province (18030701185), the Academic and Technical Talents and the Back-up Candidates Funding for Scientific Research Activities of Anhui Province (2016H093), the Open Foundation of State Key Laboratory of Agrobiotechnology (2018SKLAB6-3) and the Open Fund of State Key Laboratory of Genetic Resources and Evolution (GREKF18-16).

REFERENCES

1. Conti M, Franciosi F. Acquisition of oocyte competence to develop as an embryo: integrated nuclear and cytoplasmic events. *Hum Reprod Update*. 2018; 24:245–66. <https://doi.org/10.1093/humupd/dmx040> PMID:29432538
2. Russell DL, Gilchrist RB, Brown HM, Thompson JG. Bidirectional communication between cumulus cells and the oocyte: old hands and new players? *Theriogenology*. 2016; 86:62–68.

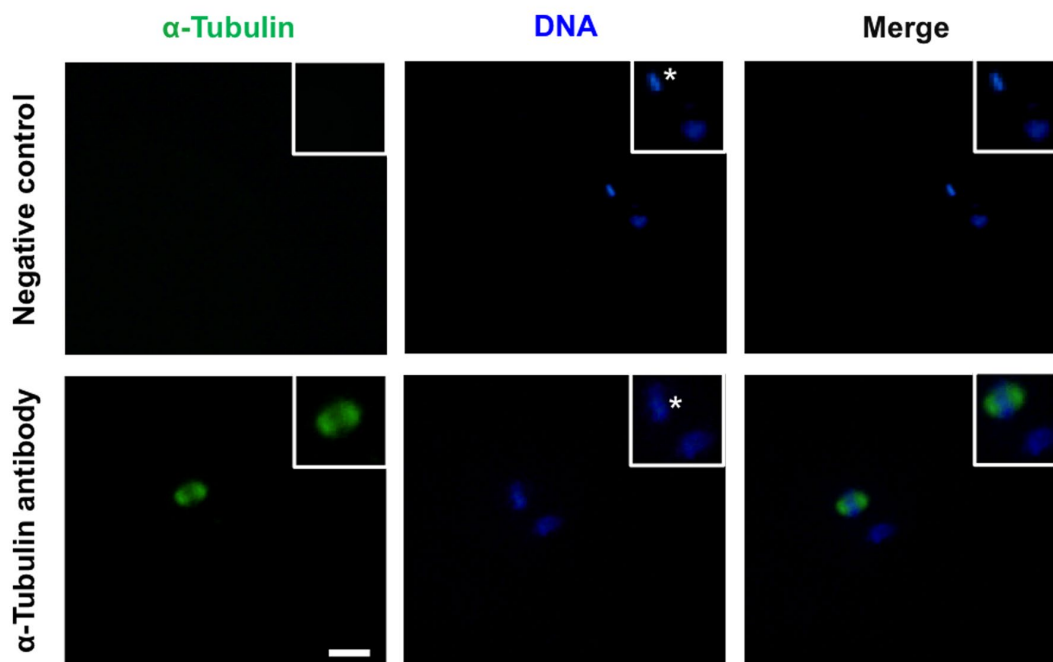
- <https://doi.org/10.1016/j.theriogenology.2016.04.019>
PMID:[27160446](https://pubmed.ncbi.nlm.nih.gov/27160446/)
3. Gilchrist RB, Ritter LJ, Armstrong DT. Oocyte-somatic cell interactions during follicle development in mammals. *Anim Reprod Sci.* 2004; 82-83:431–46.
<https://doi.org/10.1016/j.anireprosci.2004.05.017>
PMID:[15271471](https://pubmed.ncbi.nlm.nih.gov/15271471/)
 4. Gilchrist RB, Lane M, Thompson JG. Oocyte-secreted factors: regulators of cumulus cell function and oocyte quality. *Hum Reprod Update.* 2008; 14:159–77.
<https://doi.org/10.1093/humupd/dmm040>
PMID:[18175787](https://pubmed.ncbi.nlm.nih.gov/18175787/)
 5. Nagai T. The improvement of in vitro maturation systems for bovine and porcine oocytes. *Theriogenology.* 2001; 55:1291–301.
[https://doi.org/10.1016/S0093-691X\(01\)00483-6](https://doi.org/10.1016/S0093-691X(01)00483-6)
PMID:[11327685](https://pubmed.ncbi.nlm.nih.gov/11327685/)
 6. Yuan Y, Spate LD, Redel BK, Tian Y, Zhou J, Prather RS, Roberts RM. Quadrupling efficiency in production of genetically modified pigs through improved oocyte maturation. *Proc Natl Acad Sci USA.* 2017; 114:E5796–804.
<https://doi.org/10.1073/pnas.1703998114>
PMID:[28673989](https://pubmed.ncbi.nlm.nih.gov/28673989/)
 7. Prather RS, Ross JW, Isom SC, Green JA. Transcriptional, post-transcriptional and epigenetic control of porcine oocyte maturation and embryogenesis. *Soc Reprod Fertil Suppl.* 2009; 66:165–76.
PMID:[19848279](https://pubmed.ncbi.nlm.nih.gov/19848279/)
 8. Sun QY, Nagai T. Molecular mechanisms underlying pig oocyte maturation and fertilization. *J Reprod Dev.* 2003; 49:347–59.
<https://doi.org/10.1262/jrd.49.347> PMID:[14967910](https://pubmed.ncbi.nlm.nih.gov/14967910/)
 9. Dallaire A, Simard MJ. The implication of microRNAs and endo-siRNAs in animal germline and early development. *Dev Biol.* 2016; 416:18–25.
<https://doi.org/10.1016/j.ydbio.2016.06.007>
PMID:[27287880](https://pubmed.ncbi.nlm.nih.gov/27287880/)
 10. Li X, Wang H, Sheng Y, Wang Z. MicroRNA-224 delays oocyte maturation through targeting Ptx3 in cumulus cells. *Mech Dev.* 2017; 143:20–25.
<https://doi.org/10.1016/j.mod.2016.12.004>
PMID:[28039065](https://pubmed.ncbi.nlm.nih.gov/28039065/)
 11. Wright EC, Hale BJ, Yang CX, Njoka JG, Ross JW. MicroRNA-21 and PDCD4 expression during in vitro oocyte maturation in pigs. *Reprod Biol Endocrinol.* 2016; 14:21–31.
<https://doi.org/10.1186/s12958-016-0152-2>
PMID:[27084064](https://pubmed.ncbi.nlm.nih.gov/27084064/)
 12. Gay S, Bugeon J, Bouchareb A, Henry L, Delahaye C, Legeai F, Montfort J, Le Cam A, Siegel A, Bobe J, Thermes V. MiR-202 controls female fecundity by regulating medaka oogenesis. *PLoS Genet.* 2018; 14:e1007593.
<https://doi.org/10.1371/journal.pgen.1007593>
PMID:[30199527](https://pubmed.ncbi.nlm.nih.gov/30199527/)
 13. Minogue AL, Tackett MR, Atabakhsh E, Tejada G, Arur S. Functional genomic analysis identifies miRNA repertoire regulating *C. elegans* oocyte development. *Nat Commun.* 2018; 9:5318–28.
<https://doi.org/10.1038/s41467-018-07791-w>
PMID:[30552320](https://pubmed.ncbi.nlm.nih.gov/30552320/)
 14. Suh N, Baehner L, Moltzahn F, Melton C, Shenoy A, Chen J, Belloch R. MicroRNA function is globally suppressed in mouse oocytes and early embryos. *Curr Biol.* 2010; 20:271–77.
<https://doi.org/10.1016/j.cub.2009.12.044>
PMID:[20116247](https://pubmed.ncbi.nlm.nih.gov/20116247/)
 15. Taylor DH, Chu ET, Spektor R, Soloway PD. Long non-coding RNA regulation of reproduction and development. *Mol Reprod Dev.* 2015; 82:932–56.
<https://doi.org/10.1002/mrd.22581>
PMID:[26517592](https://pubmed.ncbi.nlm.nih.gov/26517592/)
 16. Lasda E, Parker R. Circular RNAs: diversity of form and function. *RNA.* 2014; 20:1829–42.
<https://doi.org/10.1261/rna.047126.114>
PMID:[25404635](https://pubmed.ncbi.nlm.nih.gov/25404635/)
 17. Fan X, Zhang X, Wu X, Guo H, Hu Y, Tang F, Huang Y. Single-cell RNA-seq transcriptome analysis of linear and circular RNAs in mouse preimplantation embryos. *Genome Biol.* 2015; 16:148–64.
<https://doi.org/10.1186/s13059-015-0706-1>
PMID:[26201400](https://pubmed.ncbi.nlm.nih.gov/26201400/)
 18. Liang G, Yang Y, Niu G, Tang Z, Li K. Genome-wide profiling of *Sus scrofa* circular RNAs across nine organs and three developmental stages. *DNA Res.* 2017; 24:523–35.
<https://doi.org/10.1093/dnares/dsx022>
PMID:[28575165](https://pubmed.ncbi.nlm.nih.gov/28575165/)
 19. Shen M, Li T, Zhang G, Wu P, Chen F, Lou Q, Chen L, Yin X, Zhang T, Wang J. Dynamic expression and functional analysis of circRNA in granulosa cells during follicular development in chicken. *BMC Genomics.* 2019; 20:96–100.
<https://doi.org/10.1186/s12864-019-5462-2>
PMID:[30700247](https://pubmed.ncbi.nlm.nih.gov/30700247/)
 20. Bose R, Ain R. Regulation of Transcription by Circular RNAs. *Adv Exp Med Biol.* 2018; 1087:81–94.
https://doi.org/10.1007/978-981-13-1426-1_7
PMID:[30259359](https://pubmed.ncbi.nlm.nih.gov/30259359/)
 21. Suzuki H, Tsukahara T. A view of pre-mRNA splicing from RNase R resistant RNAs. *Int J Mol Sci.* 2014; 15:9331–42.

- <https://doi.org/10.3390/ijms15069331>
PMID:[24865493](https://pubmed.ncbi.nlm.nih.gov/24865493/)
22. Dang Y, Yan L, Hu B, Fan X, Ren Y, Li R, Lian Y, Yan J, Li Q, Zhang Y, Li M, Ren X, Huang J, et al. Tracing the expression of circular RNAs in human pre-implantation embryos. *Genome Biol.* 2016; 17:130–44.
<https://doi.org/10.1186/s13059-016-0991-3>
PMID:[27315811](https://pubmed.ncbi.nlm.nih.gov/27315811/)
23. Cai H, Li Y, Li H, Niringiyumukiza JD, Zhang M, Chen L, Chen G, Xiang W. Identification and characterization of human ovary-derived circular RNAs and their potential roles in ovarian aging. *Aging (Albany NY).* 2018; 10:2511–34.
<https://doi.org/10.18632/aging.101565>
PMID:[30260796](https://pubmed.ncbi.nlm.nih.gov/30260796/)
24. Chen X, Shi W, Chen C. Differential circular RNAs expression in ovary during oviposition in honey bees. *Genomics.* 2019; 111:598–606.
<https://doi.org/10.1016/j.ygeno.2018.03.015>
PMID:[29709513](https://pubmed.ncbi.nlm.nih.gov/29709513/)
25. Dong WW, Li HM, Qing XR, Huang DH, Li HG. Identification and characterization of human testis derived circular RNAs and their existence in seminal plasma. *Sci Rep.* 2016; 6:39080–90.
<https://doi.org/10.1038/srep39080> PMID:[27958373](https://pubmed.ncbi.nlm.nih.gov/27958373/)
26. Gao Y, Wu M, Fan Y, Li S, Lai Z, Huang Y, Lan X, Lei C, Chen H, Dang R. Identification and characterization of circular RNAs in Qinchuan cattle testis. *R Soc Open Sci.* 2018; 5:180413–22.
<https://doi.org/10.1098/rsos.180413>
PMID:[30109096](https://pubmed.ncbi.nlm.nih.gov/30109096/)
27. Yan L, Feng J, Cheng F, Cui X, Gao L, Chen Y, Wang F, Zhong T, Li Y, Liu L. Circular RNA expression profiles in placental villi from women with gestational diabetes mellitus. *Biochem Biophys Res Commun.* 2018; 498:743–50.
<https://doi.org/10.1016/j.bbrc.2018.03.051>
PMID:[29526755](https://pubmed.ncbi.nlm.nih.gov/29526755/)
28. Tao H, Xiong Q, Zhang F, Zhang N, Liu Y, Suo X, Li X, Yang Q, Chen M. Circular RNA profiling reveals chi_circ_0008219 function as microRNA sponges in pre-ovulatory ovarian follicles of goats (*Capra hircus*). *Genomics.* 2017; 17:30129–35.
<https://doi.org/10.1016/j.ygeno.2017.10.005>
PMID:[29107014](https://pubmed.ncbi.nlm.nih.gov/29107014/)
29. Lin X, Han M, Cheng L, Chen J, Zhang Z, Shen T, Wang M, Wen B, Ni T, Han C. Expression dynamics, relationships, and transcriptional regulations of diverse transcripts in mouse spermatogenic cells. *RNA Biol.* 2016; 13:1011–24.
<https://doi.org/10.1080/15476286.2016.1218588>
PMID:[27560004](https://pubmed.ncbi.nlm.nih.gov/27560004/)
30. Fu Y, Jiang H, Liu JB, Sun XL, Zhang Z, Li S, Gao Y, Yuan B, Zhang JB. Genome-wide analysis of circular RNAs in bovine cumulus cells treated with BMP15 and GDF9. *Sci Rep.* 2018; 8:7944.
<https://doi.org/10.1038/s41598-018-26157-2>
PMID:[29786687](https://pubmed.ncbi.nlm.nih.gov/29786687/)
31. Cheng J, Huang J, Yuan S, Zhou S, Yan W, Shen W, Chen Y, Xia X, Luo A, Zhu D, Wang S. Circular RNA expression profiling of human granulosa cells during maternal aging reveals novel transcripts associated with assisted reproductive technology outcomes. *PLoS One.* 2017; 12:e0177888.
<https://doi.org/10.1371/journal.pone.0177888>
PMID:[28644873](https://pubmed.ncbi.nlm.nih.gov/28644873/)
32. Yu CY, Li TC, Wu YY, Yeh CH, Chiang W, Chuang CY, Kuo HC. The circular RNA circBIRC6 participates in the molecular circuitry controlling human pluripotency. *Nat Commun.* 2017; 8:1149–63.
<https://doi.org/10.1038/s41467-017-01216-w>
PMID:[29074849](https://pubmed.ncbi.nlm.nih.gov/29074849/)
33. Lei W, Feng T, Fang X, Yu Y, Yang J, Zhao ZA, Liu J, Shen Z, Deng W, Hu S. Signature of circular RNAs in human induced pluripotent stem cells and derived cardiomyocytes. *Stem Cell Res Ther.* 2018; 9:56–68.
<https://doi.org/10.1186/s13287-018-0793-5>
PMID:[29523209](https://pubmed.ncbi.nlm.nih.gov/29523209/)
34. Li X, Ao J, Wu J. Systematic identification and comparison of expressed profiles of lncRNAs and circRNAs with associated co-expression and ceRNA networks in mouse germline stem cells. *Oncotarget.* 2017; 8:26573–90.
<https://doi.org/10.18632/oncotarget.15719>
PMID:[28404936](https://pubmed.ncbi.nlm.nih.gov/28404936/)
35. Gardner EJ, Nizami ZF, Talbot CC Jr, Gall JG. Stable intronic sequence RNA (sisRNA), a new class of noncoding RNA from the oocyte nucleus of *Xenopus tropicalis*. *Genes Dev.* 2012; 26:2550–59.
<https://doi.org/10.1101/gad.202184.112>
PMID:[23154985](https://pubmed.ncbi.nlm.nih.gov/23154985/)
36. Venø MT, Hansen TB, Venø ST, Clausen BH, Grebing M, Finsen B, Holm IE, Kjems J. Spatio-temporal regulation of circular RNA expression during porcine embryonic brain development. *Genome Biol.* 2015; 16:245–61.
<https://doi.org/10.1186/s13059-015-0801-3>
PMID:[26541409](https://pubmed.ncbi.nlm.nih.gov/26541409/)
37. Kulcheski FR, Christoff AP, Margis R. Circular RNAs are miRNA sponges and can be used as a new class of biomarker. *J Biotechnol.* 2016; 238:42–51.
<https://doi.org/10.1016/j.jbiotec.2016.09.011>
PMID:[27671698](https://pubmed.ncbi.nlm.nih.gov/27671698/)
38. Pan B, Toms D, Shen W, Li J. MicroRNA-378 regulates oocyte maturation via the suppression of aromatase in

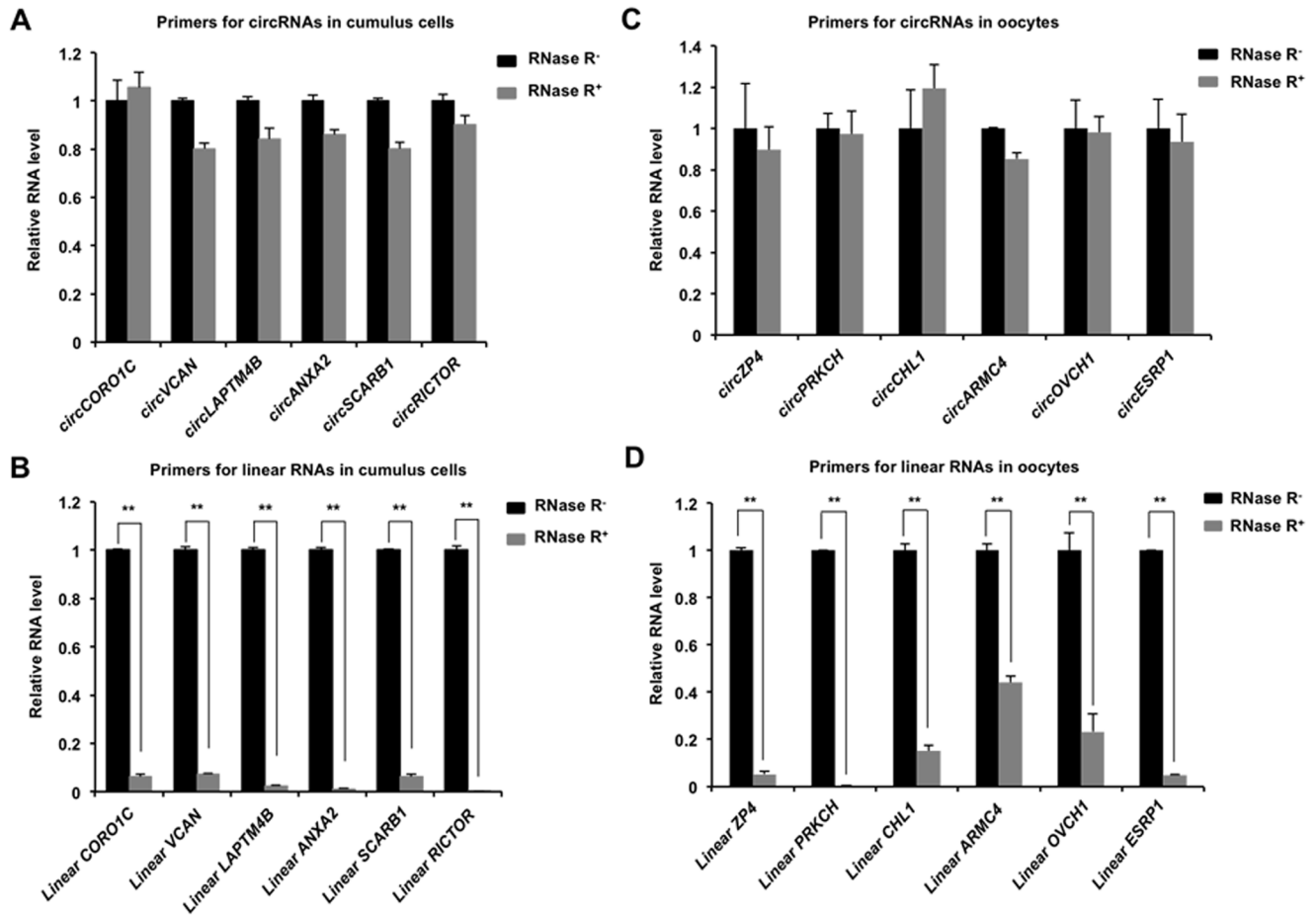
- porcine cumulus cells. *Am J Physiol Endocrinol Metab.* 2015; 308:E525–34.
<https://doi.org/10.1152/ajpendo.00480.2014>
 PMID:[25628423](https://pubmed.ncbi.nlm.nih.gov/25628423/)
39. Vo JN, Cieslik M, Zhang Y, Shukla S, Xiao L, Zhang Y, Wu YM, Dhanasekaran SM, Engelke CG, Cao X, Robinson DR, Nesvizhskii AI, Chinnaiyan AM. The Landscape of Circular RNA in Cancer. *Cell.* 2019; 176:869–881.e13.
<https://doi.org/10.1016/j.cell.2018.12.021>
 PMID:[30735636](https://pubmed.ncbi.nlm.nih.gov/30735636/)
 40. Reyes JM, Ross PJ. Cytoplasmic polyadenylation in mammalian oocyte maturation. *Wiley Interdiscip Rev RNA.* 2016; 7:71–89.
<https://doi.org/10.1002/wrna.1316>
 PMID:[26596258](https://pubmed.ncbi.nlm.nih.gov/26596258/)
 41. Oliveira AF, Yasuda R. Imaging the activity of Ras superfamily GTPase proteins in small subcellular compartments in neurons. *Methods Mol Biol.* 2014; 1071:109–28.
https://doi.org/10.1007/978-1-62703-622-1_9
 PMID:[24052384](https://pubmed.ncbi.nlm.nih.gov/24052384/)
 42. Fukata M, Kaibuchi K. Rho-family GTPases in cadherin-mediated cell-cell adhesion. *Nat Rev Mol Cell Biol.* 2001; 2:887–97.
<https://doi.org/10.1038/35103068>
 PMID:[11733768](https://pubmed.ncbi.nlm.nih.gov/11733768/)
 43. Jiang C, Diao F, Sang YJ, Xu N, Zhu RL, Wang XX, Chen Z, Tao WW, Yao B, Sun HX, Huang XX, Xue B, Li CJ. GGPP-Mediated Protein Geranylgeranylation in Oocyte Is Essential for the Establishment of Oocyte-Granulosa Cell Communication and Primary-Secondary Follicle Transition in Mouse Ovary. *PLoS Genet.* 2017; 13:e1006535.
<https://doi.org/10.1371/journal.pgen.1006535>
 PMID:[28072828](https://pubmed.ncbi.nlm.nih.gov/28072828/)
 44. Schuster MK, Schmierer B, Shkumatava A, Kuchler K. Activin A and follicle-stimulating hormone control tight junctions in avian granulosa cells by regulating occludin expression. *Biol Reprod.* 2004; 70:1493–99.
<https://doi.org/10.1095/biolreprod.103.024331>
 PMID:[14736813](https://pubmed.ncbi.nlm.nih.gov/14736813/)
 45. Zhang Y, Duan X, Cao R, Liu HL, Cui XS, Kim NH, Rui R, Sun SC. Small GTPase RhoA regulates cytoskeleton dynamics during porcine oocyte maturation and early embryo development. *Cell Cycle.* 2014; 13:3390–403.
<https://doi.org/10.4161/15384101.2014.952967>
 PMID:[25485583](https://pubmed.ncbi.nlm.nih.gov/25485583/)
 46. Li M, Liang CG, Xiong B, Xu BZ, Lin SL, Hou Y, Chen DY, Schatten H, Sun QY. PI3-kinase and mitogen-activated protein kinase in cumulus cells mediate EGF-induced meiotic resumption of porcine oocyte. *Domest Anim Endocrinol.* 2008; 34:360–71.
<https://doi.org/10.1016/j.domaniend.2007.10.001>
 PMID:[18023131](https://pubmed.ncbi.nlm.nih.gov/18023131/)
 47. Hanna CB, Yao S, Patta MC, Jensen JT, Wu X. WEE2 is an oocyte-specific meiosis inhibitor in rhesus macaque monkeys. *Biol Reprod.* 2010; 82:1190–97.
<https://doi.org/10.1095/biolreprod.109.081984>
 PMID:[20200212](https://pubmed.ncbi.nlm.nih.gov/20200212/)
 48. Ramos Leal G, Santos Monteiro CA, Souza-Fabjan JM, de Paula Vasconcelos CO, Garcia Nogueira LA, Reis Ferreira AM, Varella Serapião R. Role of cAMP modulator supplementations during oocyte in vitro maturation in domestic animals. *Anim Reprod Sci.* 2018; 199:1–14.
<https://doi.org/10.1016/j.anireprosci.2018.11.002>
 PMID:[30449707](https://pubmed.ncbi.nlm.nih.gov/30449707/)
 49. Luo H, Kimura K, Aoki M, Hirako M. Effect of vascular endothelial growth factor on maturation, fertilization and developmental competence of bovine oocytes. *J Vet Med Sci.* 2002; 64:803–06.
<https://doi.org/10.1292/jvms.64.803> PMID:[12399605](https://pubmed.ncbi.nlm.nih.gov/12399605/)
 50. Yan L, Luo H, Gao X, Liu K, Zhang Y. Vascular endothelial growth factor-induced expression of its receptors and activation of the MAPK signaling pathway during ovine oocyte maturation in vitro. *Theriogenology.* 2012; 78:1350–60.
<https://doi.org/10.1016/j.theriogenology.2012.06.001>
 PMID:[22898011](https://pubmed.ncbi.nlm.nih.gov/22898011/)
 51. Bui TM, Nguyễn KX, Karata A, Ferré P, Trần MT, Wakai T, Funahashi H. Presence of vascular endothelial growth factor during the first half of IVM improves the meiotic and developmental competence of porcine oocytes from small follicles. *Reprod Fertil Dev.* 2017; 29:1902–09.
<https://doi.org/10.1071/RD16321> PMID:[27938625](https://pubmed.ncbi.nlm.nih.gov/27938625/)
 52. Webster RJ, Giles KM, Price KJ, Zhang PM, Mattick JS, Leedman PJ. Regulation of epidermal growth factor receptor signaling in human cancer cells by microRNA-7. *J Biol Chem.* 2009; 284:5731–41.
<https://doi.org/10.1074/jbc.M804280200>
 PMID:[19073608](https://pubmed.ncbi.nlm.nih.gov/19073608/)
 53. Prochazka R, Blaha M, Nemcová L. Significance of epidermal growth factor receptor signaling for acquisition of meiotic and developmental competence in mammalian oocytes. *Biol Reprod.* 2017; 97:537–49.
<https://doi.org/10.1093/biolre/iox112> PMID:[29025011](https://pubmed.ncbi.nlm.nih.gov/29025011/)
 54. Cheng W, Ip YT, Xu Z. Gudu, an Armadillo repeat-containing protein, is required for spermatogenesis in *Drosophila*. *Gene.* 2013; 531:294–300.
<https://doi.org/10.1016/j.gene.2013.08.080>
 PMID:[24055424](https://pubmed.ncbi.nlm.nih.gov/24055424/)

SUPPLEMENTARY MATERIALS

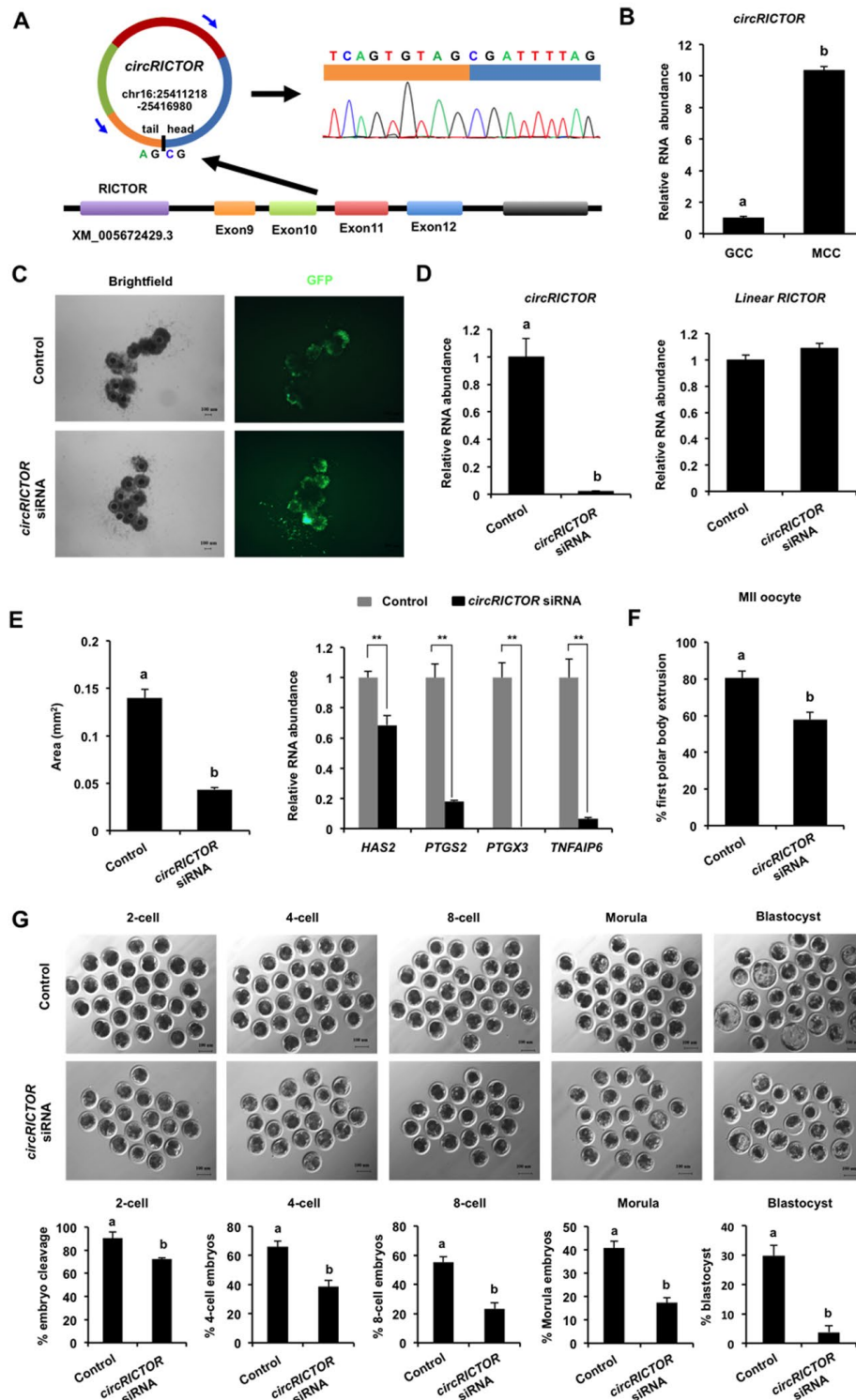
Supplementary Figures



Supplementary Figure 1. Validation of the specificity of α -tubulin antibody. MII oocytes were incubated with the diluent α -tubulin antibody in the immunofluorescence staining protocol while MII oocytes incubated with the mouse serum (Yeasen, 36118ES03) replacing α -tubulin antibody serve as a negative control. DNA was stained with DAPI (blue). Shown are representative images obtained using confocal laser-scanning microscopy. Right panel in each group shows the merged images between α -TUBULIN and DNA. White square insets indicate both spindles and chromosomes at high magnification. Asterisks mark chromosomes. Scale bar: 50 μ m.



Supplementary Figure 2. Expression of circRNAs and their corresponding linear RNAs in MCC and GV oocytes treated with or without RNase R. The several selected circRNAs and their corresponding linear RNAs were chosen from top differentially expressed circRNAs in both cumulus cells and oocytes. Total RNAs were extracted from MCC and GV oocytes, and then were treated with RNase R. The total RNAs without RNase R treatment serve as a control. Relative expression levels of the indicated circRNAs (A, C) and the corresponding linear RNAs (B, D) before and after RNase R treatment were determined by qPCR. The data were normalized against endogenous housekeeping gene *EF1α1*, and the value for both the MCC and the GV oocyte in the control group was set as one. The data are shown as mean ± S.E.M. Statistical analysis was performed using *t*-student test. Values with asterisks vary significantly, ***P* < 0.01.



Supplementary Figure 3. Effect of *circRICTOR* knockdown in cumulus cells on oocyte meiotic maturation and early embryo development. (A) Schematic illustration showed the RICTOR exon 9, 10, 11 and 15 circularization forming *circRICTOR* (blue arrow). The presence of *circRICTOR* was validated by qPCR, followed by Sanger sequencing. Black arrow represents “head-to-tail” *circRICTOR* splicing sites. (B) *CircRICTOR* expression in cumulus cells before and after oocyte maturation. (C) Representative images of cumulus-oocyte complexes transfected by lentivirus. (D) Expression levels of *circRICTOR* and linear *RICTOR* in cumulus cells after oocyte maturation. (E) Effect of *circRICTOR* knockdown on the expression of genes associated with cumulus expansion. The data are shown as mean \pm S.E.M. Statistical analysis was performed using *t*-student test. Values with asterisks or different letters vary significantly, $**P < 0.01$. (F) *circRICTOR* knockdown reduces the rate of oocyte meiotic maturation. (G) *circRICTOR* knockdown impairs early embryo development.

Supplementary Tables

Please browse Full Text version to see the data of Supplementary Table 1.

Supplementary Table 1. Porcine-specific primer and siRNA sequences used in this study.

Supplementary Table 2. Summary of sequencing results in porcine cumulus cells and oocytes at two maturational stages.

Sample name	Raw reads	Valid reads	Clean bases(G)	Clean Ratio(reads)	Q20%	Q30%	GC content%
Pre-mature COC1	55690890	54111584	8.12G	97.16	98.88	90.77	60
Pre-mature COC2	80463120	78580046	11.79G	97.66	99.04	92.89	61
Pre-mature COC3	62790698	61122920	9.17G	97.34	99.13	91.86	60
GCC1	91383614	87290862	13.09G	95.52	98.85	93.72	62
GCC2	90896402	86742610	13.01G	95.43	98.78	93.93	62
GCC3	80986920	78284342	11.74G	96.66	98.86	94.23	61
Mature COC1	60185534	58543068	8.78G	97.27	98.89	91.25	62
Mature COC2	59305888	57515622	8.63G	96.98	98.95	91.35	61
Mature COC3	58306736	56390364	8.46G	96.71	98.76	90.35	61
MCC1	59697644	57701474	8.66G	96.66	98.37	88.99	62
MCC2	63826660	62080180	9.31G	97.26	98.74	90.01	61
MCC3	67342322	65078844	9.76G	96.64	99.1	91.22	61.5
Total	830876428	803441916					

Please browse Full Text version to see the data of Supplementary Tables 3–8.

Supplementary Table 3. List of all circRNAs expressed in cumulus cells and oocytes.

Supplementary Table 4. List of host genes producing multiple circRNAs in cumulus cells and oocytes.

Supplementary Table 5. List of DEC and their host genes in cumulus cells and oocytes.

Supplementary Table 6. GO analysis of host genes producing DEC in cumulus cells and oocytes.

Supplementary Table 7. KEGG analysis of host genes producing DEC in cumulus cells and oocytes.

Supplementary Table 8. circRNA-miRNA interaction analysis.